ACS APPLIED MATERIALS & INTERFACES

Research Article

www.acsami.org

Simultaneous RGB Emitting Au Nanoclusters in Chitosan Nanoparticles for Anticancer Gene Theranostics

Amaresh Kumar Sahoo,[†] Subhamoy Banerjee,[‡] Siddhartha Sankar Ghosh,*[,†,‡] and Arun Chattopadhyay*[,†,§]

[†]Centre for Nanotechnology, [‡]Department of Biotechnology, and [§]Department of Chemistry, Indian Institute of Technology Guwahati, Guwahati - 781 039, India

Supporting Information

ABSTRACT: Advanced theranostic materials hold promise for targeted delivery of drugs, with the ability to follow the transport as well as its consequences. This should, ideally, be possible with minimum invasive surgery and having no or minimum cytotoxicity of the materials. It requires development of newer materials whose physical properties would allow for easy probe, which could carry the therapeutic molecules, which will be stable under physiological conditions, and at the same time would be able to permeate barriers to the target. We report the development of a composite consisting of highly fluorescent Au nanoclusters and the biopolymer chitosan, which could easily be converted into nanoparticles and would form a stable polyplex with suicide gene for induction of apoptosis in cervical cancer cells. The simultaneous red, green, and blue fluorescence from the nanoclusters provided convenient optical imaging and flow cytometry probes, without having to use additional dyes. Moreover, the colloidal nanocluster−polymer composite could be converted into solid film and be stored with the retention of optical properties. The pH tunable optical properties in the medium were also intact in the films that quickly dissolved in water with retention of properties.

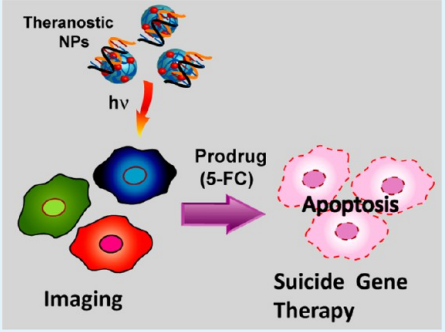

KEYWORDS: *Au nanocluster, suicide gene, bioimaging, theranostic nanoparticle*

INTRODUCTION

The ephemeral nature of noble metal nanoclusters (NCs) in liquid medium makes stabilization as the primary challenge in their syntheses.[1] Thus, while reduction of parent salt into surface plasmon resonance (SPR) active metallic nanoparticles (NPs), in the presence of a suitable stabilizing agent, has been transformed into routine exercises, the same cannot be taken for granted in the case of NCs. Here lies the need of extraordinary craftsmanship of chemistry, in the development of suitable methods for the generation of stable atomic clusters, conferred with remarkable photophysical and chemical properties. This becomes particularly important in the context of strong particle-size-dependent discretization of energy levels of clusters, as their sizes approach the Fermi wavelength of electron (ca. 0.7 nm).[2,3] Given that the discretization of energy levels, in a multielectron artificial atom model, scales with $N^{-1/3}$, where N is the number of atoms in the cluster, there seems to be an apparent fundamental disadvantage in not being able to synthesize NCs of exactly the same sizes. However, this inherent difficulty could be an advantage if one considers emission wavelength tunability in the case of particles with varied sizes. In other words, in the presence of a distribution of particles sizes, that the emission wavelengths could be different may be useful in probing biological systems, where the fluorescence inherent to the biomolecules—at several wavelengths—could otherwise interfere with the particular emission of the NCs. Further, the role of the stabilizing ligands in tuning the energy levels augurs well for the development of systematic chemistry in generating NCs with "programmed" chemical and photophysical properties.[4−6]

Among the noble metals, Au NCs are attractive, as they are potentially non-cytotoxic and the additional advantages of high fluorescence quantum yield, low photobleaching, and large Stokes-shifted emission make them a preferred choice as multicolored dye for sensitive biolabeling and bioimaging *in vivo* as well as *in vitro*.[7−9] Further, their fluorescence lifetime is useful in resolving their emission from cellular autofluorescence, which is essential in bioimaging.[10] In addition, these small clusters have high potential for chemical and photochemical catalysis.[11−13] As a consequence of their high potential for applications, a growing number of methods are being reported in the literature, which consists primarily of their synthesis in the presence of various stabilizing agents. They involve reduction of the parent salt and stabilization of the product NCs, using species such as dendrimers, DNA, proteins, polymers, and polyelectrolytes.[14−16] Typical reaction conditions invoke prolonged incubation time (~24 h), high pH, and elevated temperatures; in some cases, addition of an extra reducing agent is necessary.[17−20] Further, chemical etching of larger Au NPs (>3 nm) leading to the formation of NCs has

Received: November 14, 2013
Accepted: November 26, 2013
Published: November 26, 2013

Scheme 1. Scheme for the Synthesis of Highly Fluorescent Au Nanoclusters (NCs) for Theranostic Application[a]

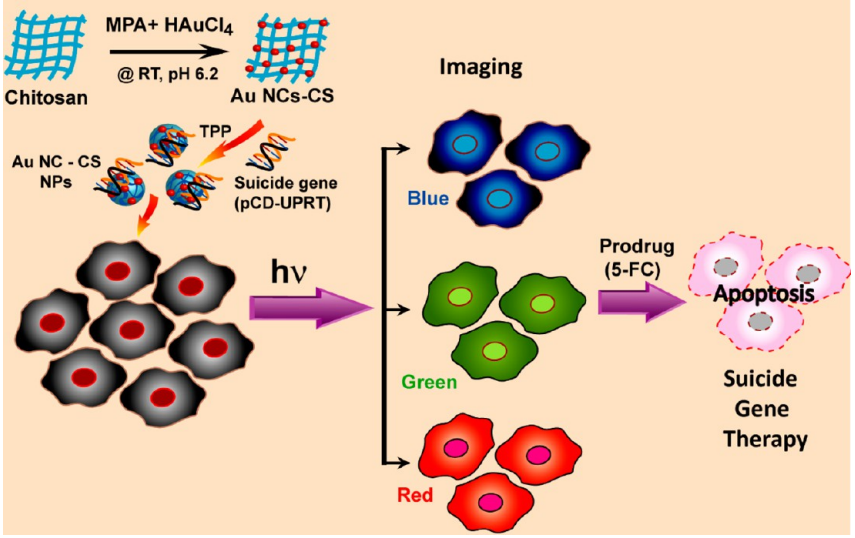

[a]The NCs were synthesized in aqueous medium by reacting $HAuCl_4$ and biopolymer chitosan at room temperature in the presence of mercaptopropionic acid. The composite was converted into nanoparticles (NPs) using tripolyphosphate, with retention of fluorescent property. Addition of the suicide gene (pCD−UPRT) to the NPs led to stable polyplex formation, which was used for induction of apoptosis in the transfected cells, following addition of prodrug 5-FC. The presence of Au NCs in the composite NPs helped in bio-imaging in red, green, and blue colors and measurement of their cellular uptake using flow cytometry, without having to use addition dyes.

been demonstrated to be a feasible option.[21−23] However, NCs produced using the reported methods are either not easily amenable to use for applications in different medium conditions or their large-scale syntheses are not viable.[24−27] In addition, the potential for applications of these novel and useful materials has not been demonstrated with clear vision, possibly because of lack of ability to maneuver the so-produced NCs. Therefore, newer methods of NC synthesis are essential, which will be convenient and produce NCs with extraordinary optical properties. Also, they should involve rather easy steps for manipulation of the products for practical applications. The favored methods ought to have the easy scale-up feasibility.

Keeping in view the issues involved in generation and use of NCs, we report here a convenient, fast, and "green" method of synthesis of red, green, and blue light emitting Au NCs, using the biopolymer chitosan, in combination with mercapto propionic acid (MPA), as the reducing agents and the stabilizers. The composite, which emitted three basic colors, could easily be turned into a chitosan nanoparticle (CS NP), favorable for facile uptake by cells,[28] and which was used as a theranostic device for induction of apoptosis in mammalian cancer cells, based on suicide gene therapy.[29] The emissions due to the NCs allowed florescence imaging using microscopy and further probe by flow cytometry (FACS), without the use of additional dyes, thereby providing an alternative to conventional dyes. The NP-mediated successful delivery of suicide gene, corresponding to *E. coli* cytosine deaminase uracil phosphoribosyltransferase (CD−UPRT) enzyme, to HeLa cells, was probed using optical emission based and other biochemical methods, which showed nanocarrier mediated gene transfection (CD−UPRT), inducing apoptosis and thus killing the cancer cells. Essentially, CD−UPRT enzyme converts non-toxic prodrug 5- fluorocytosine (5-FC) to 5-fluorouracil (5-FU) and other toxic metabolites which kill transfected cancer cells. Not only were the NCs—embedded in the polymer—stable in aqueous medium but also the composite could be converted into stable powder, in which NCs retained their emission properties. Further, the fluorescence emission of Au NCs could be changed reversibly, by varying the pH of the medium, which offered a simple way to modify the fluorescence properties of NCs, without altering their sizes. Overall, as depicted in Scheme 1, the current investigation provided a simple one step "green" synthesis of highly fluorescent Au NCs in chitosan, with multiple emission colors at various pH's and subsequent ability to modify the composite to theranostic NPs, having exclusive properties of cell imaging with generation of three basic colors inside the cell and size-limited passive targeting for cancer therapeutics.

EXPERIMENTAL SECTION

Chemicals. Chitosan (viscosity averaged molecular weight, M_v, 672 kDa and degree of deacetylation >75%), $HAuCl_4$ (Au, 17 wt % in dilute HCl; 99.99%), mercapto propionic acid (MPA), sodium tripolyphosphate (TPP), and agarose were procured from Sigma-Aldrich and used as received. Milli-Q grade water (>18 MΩ cm^{-1}, Millipore) was used in all experiments.

Synthesis of Au NCs. To synthesize the fluorescent Au NCs, chitosan solution was first prepared by dissolving 5 mg/mL in Milli-Q water containing 0.1% (v/v) acetic acid, followed by filtration to remove the residual components. The pH of the solution was then adjusted to 6.4 ± 0.2 by adding 10 M NaOH. Separately, 4 mL of water was taken in a 20 mL beaker, to which 0.5 mL of the chitosan solution (as above) was added. This was followed by addition of 40 μL of 0.11 M mercaptopropionic acid (MPA) under vigorous stirring conditions for 1 min. To this, 75 μL of 10 mM $HAuCl_4$ was added dropwise. Following addition of $HAuCl_4$, the solution was kept above a UV trans-illuminator (excitation wavelength 305 nm) after 1 min of constant stirring, for observation of color characteristic of Au NCs, which appeared right after addition of the salt.

Synthesis of Composite NPs. Composite NPs were synthesized by using the ionotropic gelation method, developed by Calvo et al., which was slightly modified herein.[30] Briefly, aqueous solution of TPP (0.2 mg/mL) was dropwise added, under stirring condition at room temperature, into previously prepared Au NC−chitosan composite (as above). Formation of an opalescent suspension indicated the synthesis of Au NC−chitosan NPs, which was also observed using a UV-trans

dx.doi.org/10.1021/am4051266 | ACS Appl. Mater. Interfaces 2014, 6, 712−724

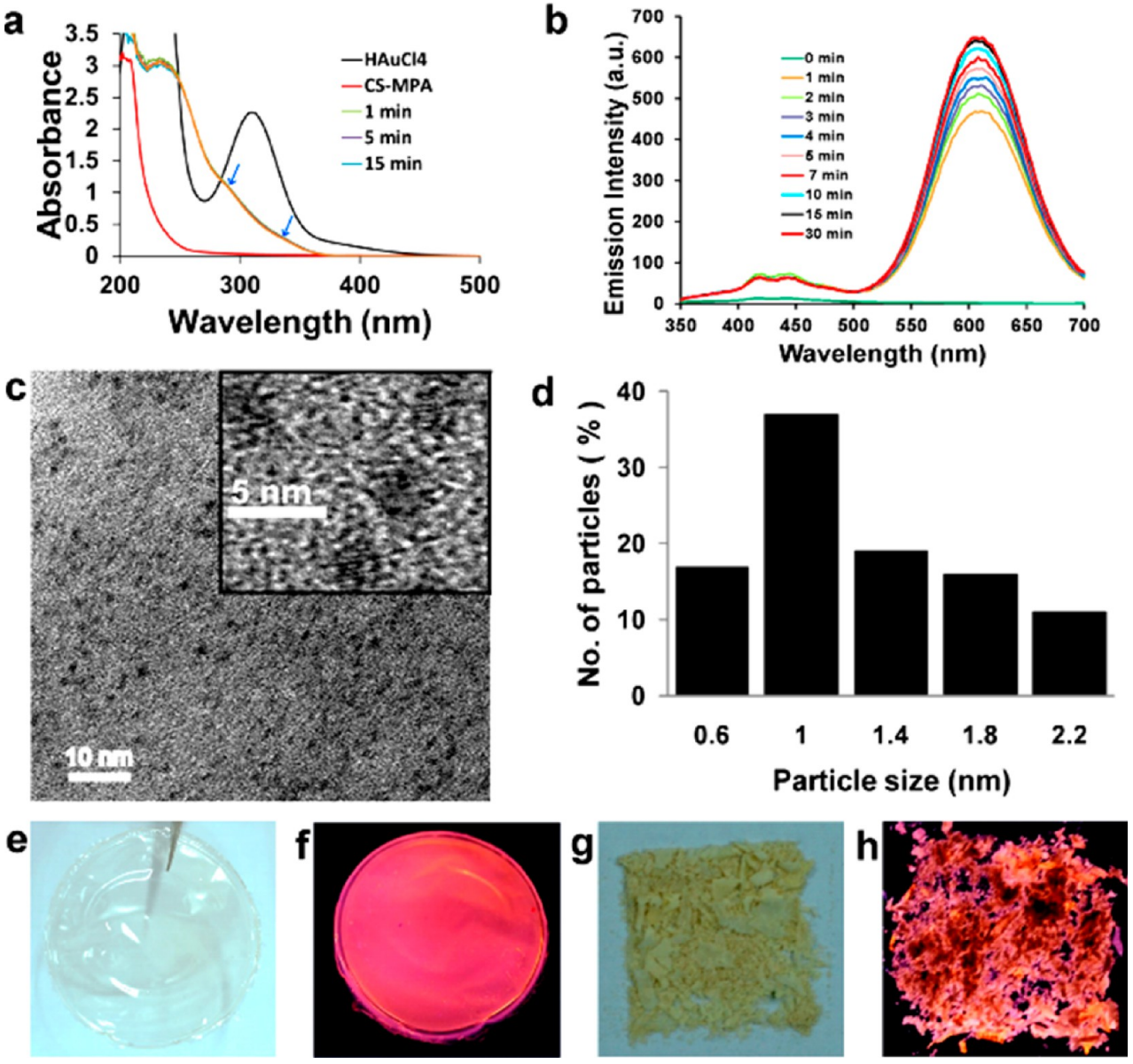

Figure 1. Characterization of Au NCs. (a) UV−vis absorption spectra recorded at different times, demonstrating the formation of Au NCs from a mixture of $HAuCl_4$ and MPA in the presence of chitosan. Also shown is the absorption spectrum of $HAuCl_4$. (b) Time-dependent emission spectra of the product (Au NCs) consisting of a major peak at 610 nm which was observed when excited by 300 nm light. (c) TEM images of the NCs. The inset shows the HRTEM images of a few such particles. (d) Particle size distribution, which was calculated on the basis of TEM images. (e) Photograph of Au NC−chitosan film recorded using visible light. The film appeared colorless and transparent. (f) Photograph of the same film recorded using UV light (305 nm). The film appeared red. (g and h) Photographs of the lyophilized Au NC−chitosan composite recorded using visible and UV light (305 nm).

illuminator. The solid composite was collected by centrifugation (6000 rpm, 5 min), which was followed by redispersion in sterile PBS buffer (pH 7.4) before using in cell culture medium. Blank chitosan NPs (without Au NCs) were synthesized by using the same method and at the same chitosan concentration (without using $HAuCl_4$) for control experiments.

Transmission Electron Microscopy (TEM). The composite and composite NPs (as-synthesized) were examined using an ultrahigh resolution transmission electron microscope (TEM; JEM 2100; Jeol, Peabody, MA, USA), operating at a maximum accelerating voltage of 200 KV. For that, 8 μL of as-synthesized composite and composite NP dispersions were separately drop-coated onto carbon-coated copper TEM grids, air-dried for 12 h, and then observed under TEM.

Fluorescence Measurements. Fluorescence experiments were carried out using fluorescence spectrophotometers LS55, Perkin-Elmer, and Fluorolog-3, Horiba Jobin Yvon, Edison, NY, USA.

Dynamic Light Scattering Study. The zeta potential and hydrodynamic diameter of the composite NPs and gene-loaded composite NPs were measured by dynamic light scattering-based analysis using a Malvern Zetasizer Nano ZS.

Matrix-Assisted Laser Desorption Ionization Time-of-Flight Mass Spectrometry (MALDI-TOF MS) Analysis. MALDI-TOF (Applied Biosystems 4800 Plus MALDI TOF/TOF Analyzer) was performed using *R*-cyano-4-hydroxycinnamic acid (CHCA) matrix.

Fourier Transform Infrared (FTIR) Spectroscopy. To perform FTIR analysis, the samples were freeze-dried (lyophilized), mixed with KBr to make the pellets, and characterized by a Perkin-Elmer Spectrum One machine in the range 4000−400 cm^{-1}.

Field-Emission Scanning Electron Microscopy (FESEM). FESEM measurements were performed in a Carl Zeiss, SIGMA VP, instrument. Typically, 20 μL of sample was drop-cast on a glass slide covered with aluminum foil, air-dried, and sputter-coated with gold

dx.doi.org/10.1021/am4051266 | ACS Appl. Mater. Interfaces 2014, 6, 712−724

film using a sputter coater (SC7620 "Mini", Polaron Sputter Coater, Quorum Technologies, Newhaven, England), before analyzing under the FESEM.

Cell Culture. HeLa cells (human cervical carcinoma) were obtained from National Center for Cell Sciences (NCCS), Pune, India, and cultured in Dulbecco's Modified Eagle's Medium supplemented with L-glutamine (4 mM), penicillin (50 units/mL), streptomycin (50 mg/mL; obtained from Sigma-Aldrich), and 10% (v/v) fetal bovine serum (obtained from PAA Laboratories, Austria) in 5% CO_2 humidified incubator at 37 °C.

Epi-Fluorescence Microscopy. For imaging, 1×10^4 HeLa cells were seeded into a six-well plate and incubated for 24 h. Cells were then treated with Au NC−chitosan NPs for 4 h and were maintained under the same conditions and medium as described above. To observe the fluorescence of NCs inside the cells, the medium was discarded; the cells were washed with 10 mM PBS and analyzed under an epi-fluorescence microscope (Nikon ECLIPSE, TS100, Tokyo). Different excitation band-pass filters such as UV (340−380 nm), blue (465−495 nm), and green (540/25 nm) and corresponding emission band-pass filters blue (435−485 nm), green (515−555 nm), and red (605/55 nm), respectively, were used in order to probe different colors of Au NCs present in the cell. To image the fluorescence of Au NCs, a nanocomposite (Au NC−chitosan) NP dispersion was drop-cast on a glass slide, air-dried, and observed using the same microscope as above.

FACS Analysis. To study the uptake of Au NC−chitosan NPs by cells, 1×10^5 HeLa cells were grown in 60 mm tissue culture dishes (BD Falcon) overnight. Then, Au NC−chitosan NPs were added and incubated for 4 and 8 h before harvesting them. To collect the cells, residual medium was removed, carefully washed with PBS, trypsinized, and collected by centrifugation (650 rcf, 5 min). The cell pellets were redispersed into cold PBS and analyzed by FACS Calibur (BD Biosciences, NJ). Fluorescence of Au NC (in the form of Au NC−chitosan NP) uptake by cells was recorded with the CellQuest pro in different fluoresce channels, including FL1 (530/30 nm), FL2 (band-pass filter, 585/42 nm), and FL3 (low pass filter, 670 nm) for 15 000 cells in each sample.

DNA Binding and DNase Protection Assays. In order to find out the DNA binding ability of NPs (Au NC−chitosan NPs), varying concentrations (0.0, 0.2, 0.5, 1.0, 2.0, and 3.0 μg) of NPs were incubated with pCD−UPRT (0.5 μg) at 37 °C for 1 h, followed by gel electrophoresis. The above-mentioned polyplexes of pDNA−NPs were used to carry out the DNase protection assay, in the presence and absence of 1 U/mL DNase I (Promega, USA) for 15 min and at 37 °C, prior to gel electrophoresis. To perform partial digestion, the working concentration of enzyme used was less than the original concentration (10 U/mL DNase I) as described by the manufacturer's protocol. The gel electrophoresis was performed in 0.8% agarose gel at 5 V/cm and was visualized in a gel documentation system.

Cell Viability Assay. To quantify the cell viability due to the delivery of suicide gene, 1×10^4 HeLa cells/well were seeded in a 96-well microtiter plate and grown overnight by maintaining the same medium and condition as described previously. Before performing the gene transfection, the cells were supplemented in serum free medium and treated with the CD−UPRT gene loaded Au NC−chitosan NPs for 6 h as well by maintaining the same physiological condition described above. Then, serum free medium was removed, washed with PBS, and redispersed in serum medium and subsequently different concentrations of 5 FC were added. After 72 h, MTT (3-(4,5-dimethylthiazolyl-2)-2,5-diphenyltetrazolium bromide) assay was performed to find out the number of viable cells. In live cells, the respiratory mitochondria reduce MTT into color formazan. Thus, the amount of formazan product (i.e., absorbance at 550 nm) is directly proportional to the number of live cells in the culture. The absorbance at 690 nm is due to background interference. The % of cell viability was calculated as below.

$$\%\ \text{viable cells} = [(A_{550} - A_{690})\ \text{of NP treated cells} / (A_{550} - A_{690})\ \text{of control cells}] \times 100$$

RESULTS AND DISCUSSION

A simple, fast, and "one-step" method has been developed to synthesize highly fluorescent Au NCs in aqueous medium, by reacting 10 mM $HAuCl_4$ and 5 mg/mL chitosan (at pH 6.3), in the presence of mercapto propionic acid (MPA) at room temperature. The reaction was virtually complete in about 1 min, following which probe revealed characteristic NC formation. The UV−vis spectrum of the colorless dispersion did not exhibit any peak in the region 400−800 nm (Figure 1a), thus excluding the formation of SPR active Au NPs. However, the spectrum consisted of peaks at 290 and 340 nm (marked by arrows in the spectrum in Figure 1a). Literature reports attribute the peaks to the formation of Au (I)−thiolate complexes, either as independent species or on the surface of clusters of Au atoms.[16,17,31−33] A control experiment, involving recording of the UV−vis spectrum of $HAuCl_4$, indicated that the peak at 310 nm is due to the $AuCl^{4-}$ ions. Additionally, the spectrum due to a mixture of chitosan plus MPA showed no peak in the region. The disappearance of the peak at 310 nm following reaction, accompanied by absence of the SPR peak of Au NPs, indicated possible conversion of the salt into Au clusters. Interestingly, the UV−vis spectrum recorded after 1, 5, and 15 min of mixing the reagents remained virtually the same, indicating that the products were possibly formed in the first 1 min of reaction and any change in the nature and amount of product might have been marginal after the first minute. Importantly, upon excitation by UV light (at 300 nm), the composite exhibited a strong emission peak at 610 nm and two comparatively weaker peaks in the region 400−450 nm (Figure 1b). The fluorescence spectrum is indicative of the formation of Au NCs, as it is similar to the characteristic spectrum of the NCs reported in the literature. Further, metallic NCs generally have large Stokes-shifted emission, which may well be the case here.[16] The excitation spectrum of the dispersion, corresponding to the emission peak at 610 nm consisted of two peaks—one at 302 nm and the other at 334 nm—which are possibly due to the Au NC and Au(I) complex,[17] respectively (refer to the Supporting Information, Figure S1a). Further, the fluorescence spectrum of the reaction medium (Figure 1b), recorded at several time points after addition of reactants, indicated the formation of product primarily in the first 1 min of reaction. The reaction appeared to be complete by 15 min, as there was no difference in emission intensities recorded at 15 and 30 min of reaction. The apparent minor difference in changes as a function of reaction time between UV−vis and fluorescence results could be due to surface passivation of the clusters that occurred in the presence of changing chemical environment of the product NCs. Generally, synthesis of NCs requires, other than harsher reaction conditions, several hours for product formation, which has been reduced to a few minutes, making the current method rather straightforward and rapid. Additionally, the fluorescence spectrum recorded over a week showed no change in product formation over the time period, indicating stable NC formation in the medium (refer to the Supporting Information, Figure S1b). That the method does not require extra steps and time for purification of NCs, usually associated with the formation of larger NPs, provides the current way a unique advantage over earlier reported methods.[34−39]

Further, TEM analysis of as-prepared sample revealed the formation of spherical nanoscale particles with nearly uniform size distribution (Figure 1c,d). The average diameter calculated from several images consisting of 100 such particles was found

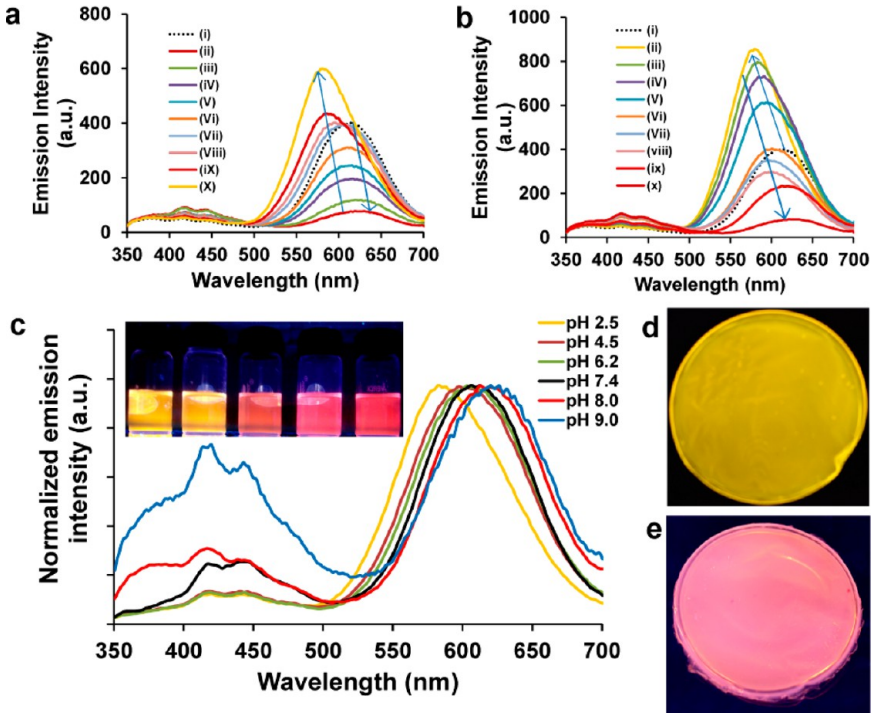

Figure 2. pH-dependent reversible changes in fluorescence of the Au NC−chitosan composite. (a, b) In both panels, the emission spectrum of as-synthesized NCs is marked by a dotted line (i). For the spectra reported in panel a, the pH of the medium of as-synthesized Au NCs was first increased by adding 0.3 M NaOH, which decreased the emission intensity with a red shift of the emission peak as in ii. To this medium, (iii) 0.1 mM, (iv) 0.3 mM, (v) 0.5 mM, (vi) 0.7 mM, (vii) 1.0 mM, (viii) 1.2 mM, (ix) 1.5 mM, and (x) 2.0 mM dilute HCl was added, which resulted in the resumption of the fluorescence intensity with gradual blue shift. On the other hand, for the spectra reported in panel b, the pH of the medium of as-synthesized Au NCs was dropped first by adding 0.1 M HCl, which resulted in the increase of fluorescence intensity accompanied by blue shift of the emission peak as in ii. To this medium, (iii) 0.2 mM, (iv) 0.5 mM, (v) 0.7 mM, (vi) 1.0 mM, (vii) 1.2 mM, (viii) 1.5 mM, (ix) 2.0 mM, and (x) 2.5 mM dilute NaOH was added, which resulted in the decrease of fluorescence intensity with gradual red shifting of the emission peak. (c) Plots of pH-dependent emissions of Au NCs with intensity normalized to the maximum. In the inset, the photographs of the solutions at different pH values are shown, recorded using a UV light source (305 nm). (d, e) UV-light illuminated photographs of the composite films. The pH of the parent medium was 4.0 (d) and 7.0 (e), respectively.

to be 1.12 ± 0.43 nm. The HRTEM image (inset of Figure 1c) of the particles showed no distinct lattice spacing of single crystalline NCs. The presence of Au was further confirmed by the EDX spectrum of the particles, recorded during the TEM analysis of the same sample (refer to the Supporting Information, Figure S2). Additionally, MALDI-TOF based mass spectrometric measurement of the sample (refer to the Supporting Information, Figure S3) exhibited a weak but clear peak at 5575.44 (in addition to a strong peak due to the polymer at 3690.0), which could be assigned to $[Au_{20}(MPA)_{15} + 3Na^+ - 7H^+]^{4-}$, indicating the presence of NC with 20 Au atoms as the main cluster. There are some additional peaks appearing at lower mass (2500−3500) possibly due to fragmentation or the presence of smaller NCs. The above-mentioned results indicated the formation of Au NCs as the product of the reaction and plasmonic nanoparticles (NPs) with higher average sizes were possibly not generated in the medium. Further, the photoemission quantum yield of the NCs was measured to be 14.7% (at pH 4.2), using quinine sulfate as the reference (refer to the Supporting Information, Figure S4). This is comparable to the reported emission efficiency of Au NCs and thus indicated the generation of strongly emitting clusters.[40,41] Additionally, a photostability study revealed that the emission intensity of the NCs remained nearly unaltered under continuous exposure of irradiation. For example, the fluorescence intensity decrease rate (F/F_0) of the NCs was 0.26% per min, whereas, in the case of commonly used fluorescent dye such as rhodamine 6G, it was found to be 1.15% per min (refer to the Supporting Information, Figure S5). Importantly, the synthesized Au NCs could be stored in solid forms as powder or film, obtained after removing water by lyophilization (Figure 1e−h). Further, the fluorescence emission of the solid film and also of the same measured by dissolving in water after 1 week exhibited the same characteristic emission as that of the original as-prepared solution, pointing to the stability of the NCs in solid form (refer to the Supporting Information, Figure S6). Thus, the current method not only produced highly luminescent Au NCs but also those which could be stored in the solid form. That the NCs could be finally obtained in stable solid form and stored for use is new as far as literature report is concerned. In addition, chitosan is a non-toxic, biodegradable, and easily available derivative of natural polymer. Therefore, this fast and facile method of preparation of water-soluble highly fluorescent Au NCs could possibly be adopted for large scale production of NCs, necessary for commercial use.

Interestingly, it was observed that the luminescence of Au NCs could be reversibly tuned by altering the pH of the medium. For example, upon raising the pH from 6.3 to 9.0, the emission maximum of the major peak of as-synthesized NCs gradually shifted from 612 to 630 nm. This was accompanied by a decrease in the intensity of emission, which diminished greatly at above pH 9.0. It may be mentioned here that at higher pH chitosan is insoluble in water and thus precipitation

dx.doi.org/10.1021/am4051266 | ACS Appl. Mater. Interfaces 2014, 6, 712−724

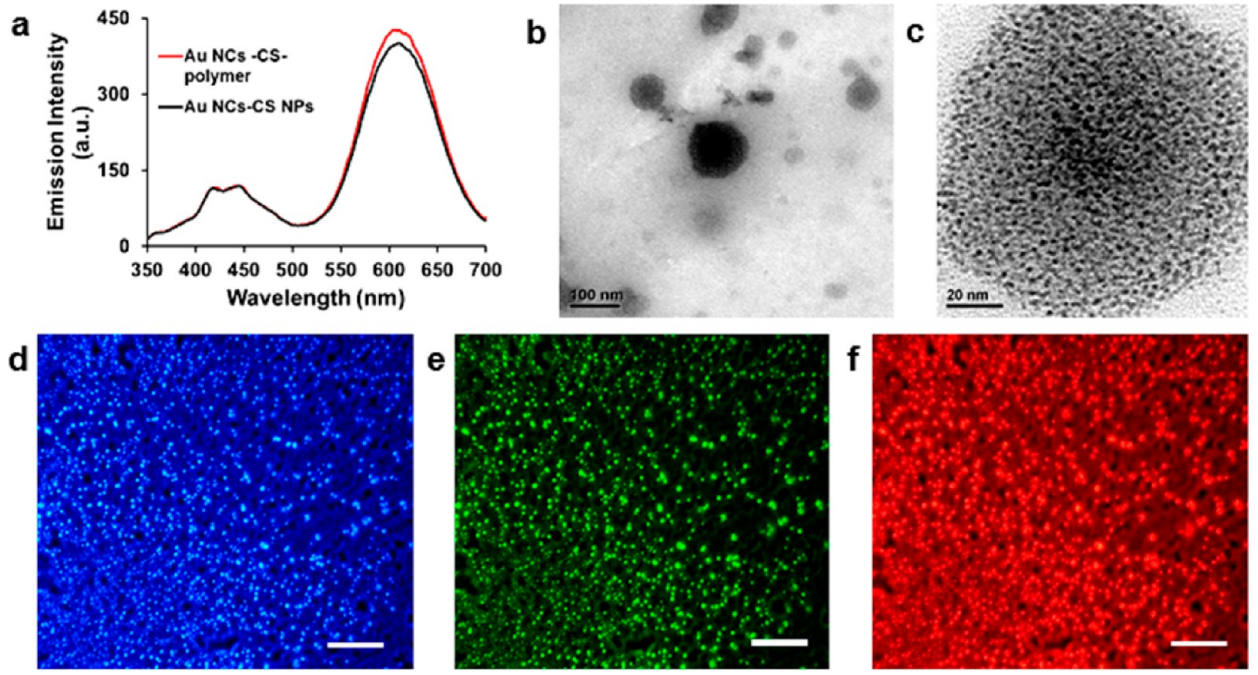

Figure 3. Characterization of the Au NC−chitosan nanoparticle. (a) Fluorescence spectra of the Au NCs (in chitosan) recorded before and after the formation of composite NPs. (b) Typical TEM inage of the composite NPs. (c) Magnified TEM image of a composite NP, which illustrated that Au NCs retained their sizes and shapes following the formation of the NPs. (d−f) Fluorescence microscopic images of the composite NPs. The composite NP-containing medium was evaporated on a glass slide in order to record the images. The three colors, namely, blue, green, and red, were observed when the sample was excited by UV, blue, and green light, respectively. The scale bar is 10 μm.

of the composite could also contribute to reduction in intensity. However, the accompanying increase in intensity of the peak occurring in the region 400−450 nm indicated the effect of pH as the primary origin of the observed changes. Further, when the pH of the solution was again made acidic by adding diluted HCl into the basic solution, the fluorescence peak reverted back to its earlier positions, and on lowering the pH below 6.3, blue shift of the emission peak was observed (Figure 2a). Separately, when the pH of the medium was adjusted to a value of 4.5 from the original 6.3, the peak not only shifted to 580 nm but also its intensity increased substantially. However, upon further decrease of pH to a value of 2.5, the intensity at 580 nm increased, without any change of the emission wavelength (Figure 2b). On the other hand, the positions of the smaller peaks (400−450 nm) remained unaltered but the intensity decreased with lowering of pH. The results indicated that not only was the fluorescence dependent on the pH of the medium but also it was reversible with respect to change in pH of the medium over a wide range (Figure 2c). Interestingly, the thin films of the composite prepared from the medium at pH 4.0 and 7.0 emitted yellow and orange colors, respectively (Figure 2d,e). The results thus indicated pH tunable emission of the clusters not only in the medium but also in solid form. It is important to mention here that a film could not be formed at higher pH as the majority of the composite settled due to insolubility of chitosan.

It may be noted here that photoluminescence of Au NCs has been explained on the basis of their size, free electron density surrounding the metal core, and also on the interactions with the species stabilizing them.[2,5,40,42] Thus, while discretization of energy bands owing to quantum confinement of electrons could primarily account for the extraordinary emission, charge transfer involving metal core, surrounding shell and surface ligands also contribute to the tunability of energy gaps. In the present case, ligand-to-metal charge transfer (LMCT) could primarily account for the change and reversibility of fluorescence based on the pH of the surrounding medium. In that context, the structure of $[Au_n(SC_2H_4COO^-)_m]$ can be considered to be consisting of a core−shell geometry with the Au core forming a −S−Au bond with the negatively charged MPA ($-SC_2H_4COO^-$). This was partly supported by FTIR spectral analysis (refer to the Supporting Information, Figure S7). Notably, the characteristic peak due to −SH stretching of MPA at~2594 cm^{-1} was absent in the FTIR spectrum of the sample. This could possibly be due to formation of a −S−Au bond. On the other hand, the peak corresponding to −CO stretching (carboxyl group) of MPA (albeit weak) and that due to −NH stretching of chitosan appeared at 1710 and at 3470 cm^{-1}, respectively.

The overall negative charge of the cluster helps it to be stabilized by the positively charged NH_3^+ group of chitosan. On the other hand, it could also be possible that the clusters were actually stabilized by both NH_3^+ groups of chitosan and $-COO^-$ groups of MPA. Thus, at acidic pH, the amine group would remain positively charged with carboxylate being neutral. On the other hand, under alkaline conditions, neutral $-NH_2$ along with $-COO^-$ of MPA would remain bound to the clusters. The difference in charges and nature of the bonds would alter the emission behavior of the NCs as a function of the pH of the medium. The exact energy levels of the clusters would, however, be dependent on the pK_a of the functional groups stabilizing them.

MALDI-TOF mass spectrometric analyses of the samples prepared at different pH's revealed that the clusters remained unaltered at different pH's. The molecular formula of the cluster remained the same at different pH's, although the degree of protonation varied, depending on the pH of the medium. For example, the mass spectral analysis indicated the

dx.doi.org/10.1021/am4051266 | ACS Appl. Mater. Interfaces 2014, 6, 712−724

presence of $[Au_{20}(MPA)_{15} + 3Na^+ - 11H^+]^{8-}$ species at pH 8.0; on the other hand, when the pH of the medium was 7.2 and 4.8, the species present were $[Au_{20}(MPA)_{15} + 3Na^+ - 7H^+]^{4-}$ and $[Au_{20}(MPA)_{15} + 3Na^+ - 4H^+]^-$, respectively (refer to the Supporting Information, Figure S3a–d). Further, measurements of zeta potential at different pH's of the medium indicated primacy of occurrence of positive charge at acidic pH (+43.9 mV at pH 4.2), whereas that was decreased to +30.3 mV at alkaline pH (9.0). The photoluminescence quantum yield of the NCs also varied with pH. For example, the maximum yield of 14.7% was observed at pH 4.2, whereas that was reduced to 8.03 and 2.51% at pH 7.4 and 9.0, respectively. It may be mentioned here that, when excited by UV light, the emission maximum due to the Au NCs varied reversibly between 580 and 630 nm, depending on the pH of the medium. Thus, a single dye quinine sulfate was deemed fit to determine QY, in this window of wavelengths, for the NC sample at different pH values. Overall, the above results indicated that the presence of chitosan and MPA as the stabilizers not only conferred stability to the NCs but also the ability to tune the optical emission based on the charge manipulation of the species present on the surface of the clusters. Thus, the material, i.e., the Au NCs with their inherently superior optical properties and the control over their emission, using charges of the stabilizing species, provided a new way of tuning their optical properties, based on acid–base chemistry of the medium. This, arguably, brings in new prospects for exploring their application potential using principles of chemistry.

An important class of applications of the brightly fluorescent, multicolor emitting, highly photostable, and potentially non-cytotoxic Au NC–chitosan composite could be in theranostics. This could involve cell imaging; this may also be delivering drug to target organ (and cells therein) with simultaneous use of the fluorescent properties for imaging. On one hand, smallness of the size of the clusters and their surface properties (if suitably modified) would allow their delivery to almost all parts of the body, including the circulatory system and cells. On the other hand, the size, structure, or charge on the polymer—at physiological pH—may not favor their transport and delivery to organs and cells easily. This includes size-selective exclusion of the polymer from entering the cell membrane. Thus, it may appear to limit the application potential of the current composite. Fortunately, chitosan polymer could be converted into NP fairly easily using the well-established ionic gelation method. It was observed that NPs of the Au NC–chitosan composite could also be formed without sacrificing the properties of the NCs. For example, the emission maximum of the composite NP was observed to be at 612 nm, when excited by 300 nm light, which was the same as that of the as-synthesized composite (Figure 3a). In addition, the QY was measured to be 6.9% (at pH 7.4) which was also close to the value of as-synthesized composite. Further, the Au NC–chitosan NPs exhibited a mean hydrodynamic diameter of 92.2 nm and zeta potential of +24 mV (refer to the Supporting Information, Figures S8a and S9). The results indicated an ideal size regime of the composite NPs which could be utilized for cellular delivery. Additionally, TEM analysis (Figure 3b,c) indicated that the average size of the composite NP was 72.1 ± 21.8 nm, which is close to the hydrodynamic diameter measured in the liquid medium and also to the average diameter measured using field emission scanning electron microscopy (FESEM, 68.5 ± 16.1 nm; refer to the Supporting Information, Figure S10). More importantly, it was observed that the average size and shape of the Au NCs remained unaffected following conversion of chitosan into NPs, i.e., the composite NPs. The observed mean size of the NCs in the composite NP was found to be 1.23 ± 0.56 nm. Thus, not only do we have a fast and convenient method of synthesis of highly fluorescent Au NCs in a biopolymer, but we also have a way of converting the bulk polymer into NPs, with NCs being embedded in them, along with retention of their optical properties. This fulfills an important requirement as far as use of the NCs in theranostic applications is concerned.

An easy and established probe for cellular indicators—be it drug delivery or functional understanding of phenomena—is based on optical imaging. In general, organic dyes are used for this purpose; they are chosen such that their emission profiles are specific to cellular regions or events, which could then easily be distinguished. In order to check the potential of the composite NPs for imaging application, they were drop-cast from the dispersion medium onto glass slides, followed by observation under an epi-fluorescence microscope. The results are shown in Figure 3d and e. As is clear from the figures, isolated particles with emission distinct from the background could be observed in all three images. More interestingly, when excited by UV, blue, and green light, the same particles could easily be observed to be emitting blue, green, and red light, respectively. This can, arguably, be considered extraordinary, as this seems to be the first report where all three basic colors are emitted by the same set of NCs. Although there are literature reports of preparation of Au NCs emitting different colors,[40,43] there are none where different colors are emitted by the same set of NCs. That the evaporated (solid) NP sample emitted color which could easily be recorded microscopically is of potentially great advantage in applying these NC containing NPs for cellular probes.

In order to test the suitability of these NPs for use as intracellular probes, human cervical cancer (HeLa) cells were incubated with 50 μg/mL of the NPs in a cell culture medium for 4 h, followed by microscopic imaging. The results are shown in Figure 4a–d. Interestingly, emissions in the form of all three basic colors, namely, blue, green, and red, could be observed to be emanating from the cells. Also, the images indicated that NPs were possibly present in both the nuclei and cytoplasm giving rise to emissions from the whole cells. Control experiments with cells only indicated that these colors were indeed due to NPs (containing Au NCs) and not from any other source. It may be noted here that cellular autofluorescence may also give rise to emission at the selected wavelength, thereby providing a false signal or interfering with the real signal. It would thus be important to find out whether such a distinction could be made in the presence of competing signals. To address this, DAPI (4′,6-diamidino-2-phenylindole, dihydrochloride), one of the widely employed nuclear staining fluorescent dyes, was used as a positive control along with the introduction of fluorescent NPs to the cells. DAPI was added 4 h after addition of the NPs to the medium. Wavelength selective excitation of the cells revealed that green and red emissions could be observed in the presence of the characteristic blue emission of DAPI (Figure 4e,f). The results not only indicated that the NCs, as delivered to the cells in the form of composite NPs, gave rise to imaging with clarity but also their emission color which could easily be discerned in the presence of parallel emissions in similar wavelength range.

An important issue that needs to be settled here is the origin of three-color emission from the same set of Au NCs present in

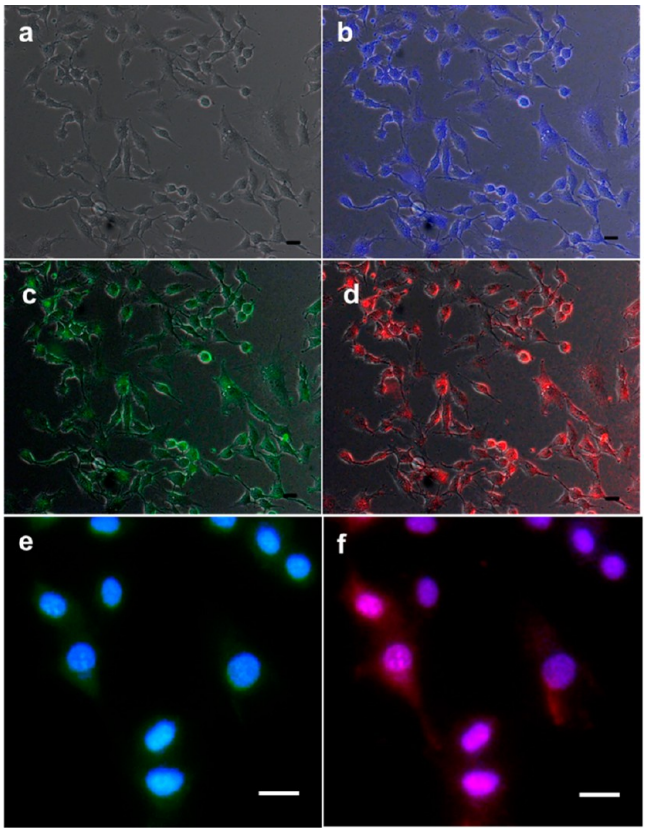

Figure 4. Fluorescence microscopic images of HeLa cells treated with Au NC−chitosan composite NPs. The images were recorded following treatment for 3 h. (a) Bright field image; (b−d) fluorescent images merged with bright field of the same cells when excited by UV, blue, and green light, respectively. (e, f) Magnified merged fluorescence images of the same cells recorded after staining with nucleus specific dye DAPI. The blue color of the stained nuclei could be observed along with the green and red fluorescence (due to the presence of Au NCs). Scale bar: 20 μm.

the NPs. As mentioned earlier, TEM investigations revealed that the Au NCs present in the composite NPs had sizes of 1.23 ± 0.56 nm. This means a considerable difference in sizes of the produced particles constituting the NCs. This could potentially be the origin, since the energy level discretization scales with $N^{-1/3}$ (N being the number of atoms in the cluster). Thus, a small difference in the particle size would mean a significant difference in the energy level separations of corresponding particles, giving rise to a significant difference in their emission wavelengths.[43−45] It should be noted here that the control experiment indicated the presence of a weak background fluorescence in the blue region due to chitosan, which became stronger following synthesis of the NCs (refer to the Supporting Information, Figure S11). This indicated the role of NCs in the emission in the blue region also.

That the three basic colors were emitted by the NCs and could be observed microscopically when present inside cells is vital to their applications in cellular imaging. However, in order for the NCs (in the composite NPs) to be useful as fluorescent probes for cellular imaging *in vivo*, they must necessarily meet the criterion of non-cytotoxicity. The test for potential cytotoxicity of the NPs was performed following the well-known 3-(4,5-dimethylthiazolyl-2)-2,5-diphenyltetrazolium bromide (MTT) assay. The results (refer to the Supporting Information, Figure S12) indicated that the NC containing NPs were not cytotoxic to mammalian cells and thus could possibly be used for imaging *in vivo*. For example, at an amount of NPs (100 μg/mL) which is double that used for imaging, there was only about 5% cell death, indicating sufficient viability of the cells in the presence of the composite NPs. It may be mentioned here that, for the last few decades, semiconductor nanocrystals otherwise known as quantum dots (Qdots) have been widely employed as cellular and *in vivo* imaging agents, replacing the traditional fluorescent organic dyes—which themselves have poor photostability and tracking lifetime.[46−48] However, apparent cytotoxicity of the majority of Qdots is limiting their large-scale use in biomedical applications.[49] On the other hand, Au NCs are not only highly fluorescent with good photostability but also non-cytotoxic. Thus, they can be considered as important candidates for replacement of existing imaging modalities during real time molecular tracking and *in vivo* imaging. In that regard, the composite NPs with embedded Au NCs would form model imaging agents.

Exclusive color emission of the Au NCs and favorable physicochemical properties of chitosan NPs prompted us to investigate the theranostic potential of the composite NPs. This was pursued by testing their ability to deliver suicide gene and kill cancer cells. Treatment of cancer continues to be a major challenge, as use of conventional chemotherapeutic agents brings in unavoidable toxicity and serious side effects due to their poor pharmacokinetics and non-specificity. It has been established that tumor tissues consist of leaky angiogenic vessels and have poor lymphatic drainage.[50−52] In this regard, NP-mediated delivery of therapeutic agents has superior potential, owing to their critical size regime allowing the particles to permeate and accumulate in tumor tissues in comparison to normal tissues. This phenomenon of passive targeting is commonly referred to as "enhanced permeability and retention (EPR)".[53] As a test case, the current NPs were employed to deliver suicide gene, which produces bifunctional cytosine deaminase−uracil phosphoribosyltransferase (CD−UPRT) enzyme, where CD converts non-toxic prodrug 5-fluorocytosine (5-FC) to toxic drug 5-fluorouracil (5-FU). Additionally, uracil phosphoribosyltransferase (UPRT), a pyrimidine salvage enzyme, converts 5-FU to other metabolites including 5-FdUMP and 5-FUTP, which inhibit DNA replication and RNA synthesis, respectively. Thus, coexpression of CD−UPRT genes ultimately leads to death of transfected cells.[54−56]

An important requirement for a viable gene delivery cargo is that it should have fairly strong interaction with the genetic material for efficient delivery to the destination, i.e., inside cells and for protection against exogenous DNase. Thus, before pursuing the experiments involving transfection of gene (CD−UPRT) into the cancer cells, the DNA binding and nuclease protection assay by the composite NPs was performed. In order to probe DNA binding efficacy, different amounts of the composite NPs were incubated with pDNA followed by agarose gel electrophoresis. The results (refer to the Supporting Information, Figure S13) revealed that the amount of pDNA migration reduced gradually with increasing concentrations of the NPs. For example, when 0.2 and 0.5 μg mL^{-1} of composite NP were added to 0.5 μg mL^{-1} pDNA, there was observable migration of DNA with lesser amount for the higher concentration of the composite (refer to the Supporting Information, Figure S13). On the other hand, for addition of 1.0, 2.0, and 3.0 μg mL^{-1} of the NP, there was no migration at all and the DNA was localized in the wells. This indicated

dx.doi.org/10.1021/am4051266 | ACS Appl. Mater. Interfaces 2014, 6, 712−724

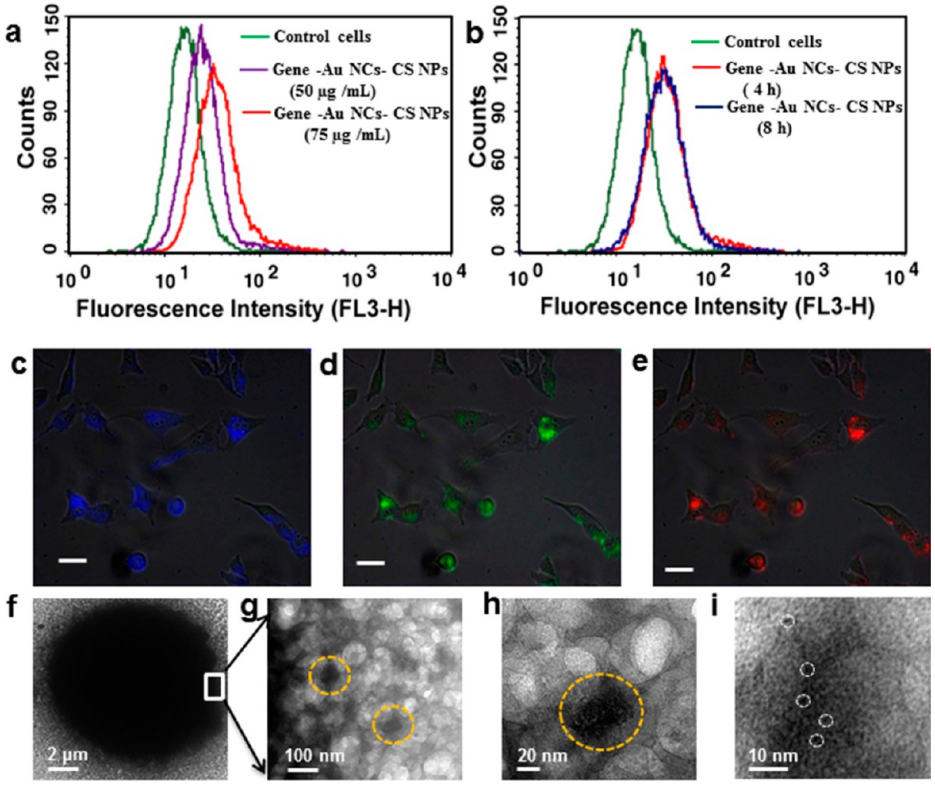

Figure 5. Suicide gene transfection of HeLa cells by gene-loaded Au NC−chitosan NPs, as followed by flow cytometry and fluorescence and transmission electron microscopy. (a) FACS analysis of HeLa cells was carried out (4 h) after transfection with different amounts of suicide gene loaded Au NC−chitosan NPs. The concentrations of the composite NPs were kept at 50 and 75 μg/mL. The results indicated dose-dependent change of fluorescence intensity in FL3-H. It may be noted here that additional dye was not used and the fluorescence from Au NCs was used for the probe. (b) For the same cells, time-dependent FACS data revealed that the fluorescence due to Au NCs present in the cells remained stable up to 8 h. (c−e) Fluorescence microscopy images merged with bright field of suicide gene loaded Au NC−chitosan NP treated cells, which showed the same three colors due to Au NCs after transfection of suicide gene in the HeLa cells. Scale bar: 20 μm. The images were recorded at 8 h following treatment of the cells. (f−i) The TEM image of the cells treated with gene-loaded NPs for 8 h. (g and h) Magnified images of cells showed the presence of composite NPs (of similar dimensions as those of as-prepared NPs) in the cells, some of which are marked with yellow circles. (i) Magnified image of one of the composite NPs showed the presence of Au NCs, some of which are marked with a white circle.

incorporation of pDNA in the composite NP and their stability when embedded in the composite. Thus, from the gel electrophoresis study, it was clear that more than 1.0 μg of Au NC−chitosan NPs was required to form a suitable polyplex with 0.5 μg of pDNA.

In order to further probe the stability of the pDNA in the composite NP, DNase protection assay was performed. The results of gel electrophoresis analysis, following treatment of the DNA-composite NP polyplex with DNase, are shown in Figure S14 of the Supporting Information. The results indicated that for a fixed concentration of DNA the intensity of the smeared band due to fragments of DNA, being produced following digestion by DNase, decreased with the increase in amount of NP, indicating stability of the DNA in the polyplex structure. For example, when the amount of composite NP was 0.2, 0.5, and 1.0 μg mL^{-1}, for the same amount of pDNA (0.6 μg mL^{-1}), there was smearing of the band but the same decreased with increased NP concentration. On the other hand, for the NP concentration of 2.0 and 3.0 μg mL^{-1}, there was no smearing. The DNA was observed to have been retained in the well, indicating protection against cleavage by the enzyme. In other words, our aim was to probe DNase activity in a comparative manner so that we would have the entire picture in one gel documentation. The optimum concentration of DNA for the formation of a stable polyplex was found to be 0.5 (μg mL^{-1}) μg^{-1} of chitosan NPs. DNase protection assay in the presence of increasing concentration of the NPs (0.2, 0.5, 1.0, 2.0, and 3.0 μg mL^{-1}, respectively) and by keeping the DNA concentration fixed (0.6 μg mL^{-1}) not only supported the stability of the polyplex but also showed clearly DNase activity for those not bound to the composite NP. Thus, the unbound DNA in a lower concentration of the NP was cleaved and formed a smear in their corresponding lanes. The amount of smearing decreased gradually with increasing amount of NPs. Hence, use of both lower and higher concentrations of composite NPs (than required for complete polyplex formation) provided a comparative view of the activity. Thus, the results demonstrated that pDNA formed a stable polyplex with composite NPs and was not susceptible to degradation by exogenous DNase.

Interestingly, following treatment with pDNA, the average hydrodynamic diameter of the Au NC−chitosan composite NP was found to have been increased from 92.2 to 159.3 nm (refer to the Supporting Information, Figure S8). The increase in diameter indicated interaction between the DNA and NP. Further, the zeta potential was measured to have decreased from +24 to +20 mV (refer to the Supporting Information, Figure S9). This possibly means an electrostatic interaction between the NP and the DNA. Chitosan is positively charged under physiological pH owing to abundance of $-NH_2^+$ moiety

dx.doi.org/10.1021/am4051266 | ACS Appl. Mater. Interfaces 2014, 6, 712−724

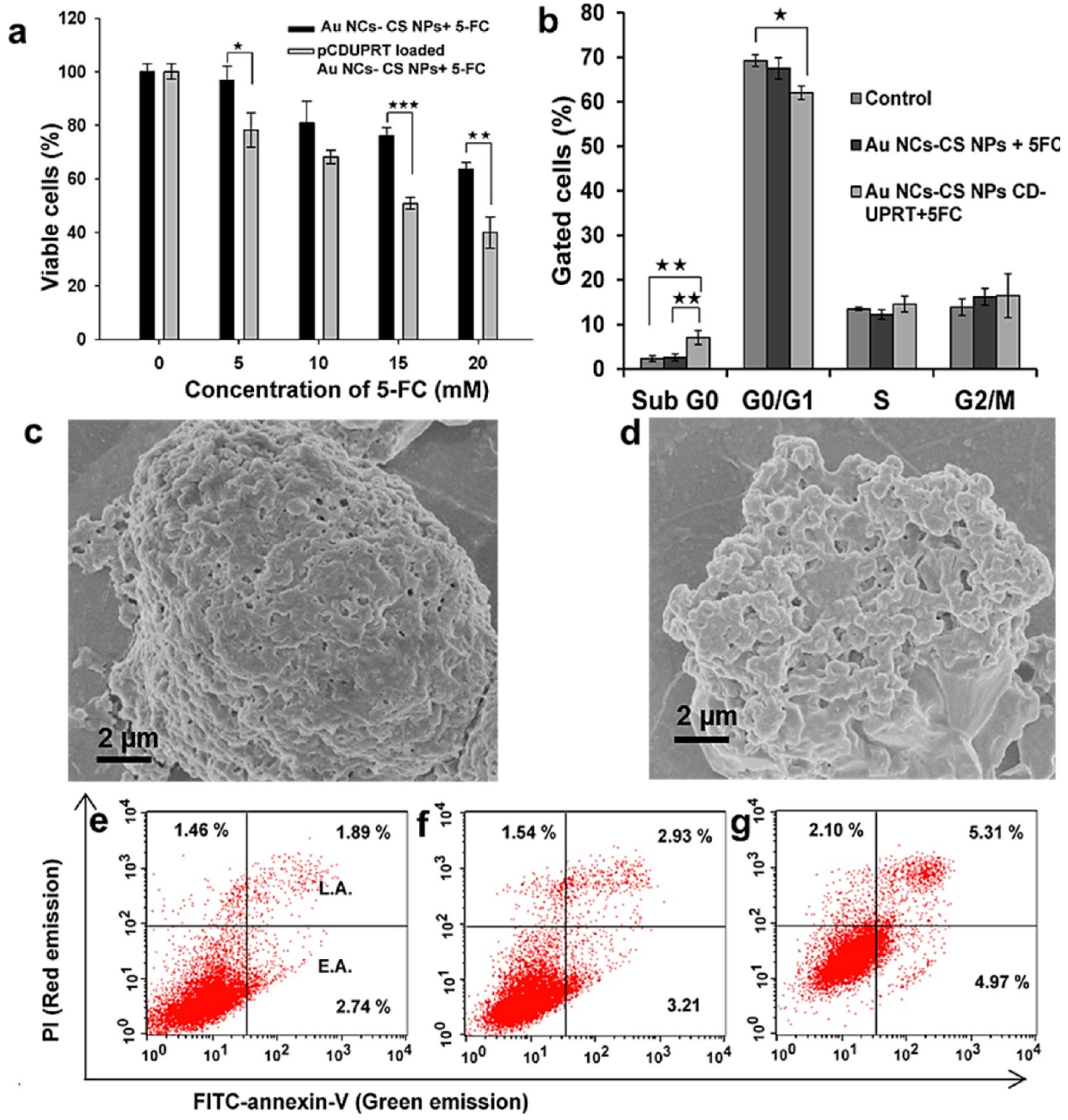

Figure 6. Apoptosis mediated cell death in the presence of the prodrug 5-FC, following functional expression of the suicide gene (CD−UPRT). (a) Cell viability, followed using MTT assay, of cells treated with 5-FC only and Au NC−chitosan NP meditated suicide gene (CD−UPRT) transfected cells following treatment with 5-FC . The values are represented as mean ± SD of results from three individual experiments. A student's *t* test was carried out to find out the statistical significance for each concentration between Au NC−chitosan NPs (blank NPs) and suicide gene (CD−UPRT) loaded Au NC−chitosan NPs after treatment with the 5-FC. The statistical significance is denoted by ★ ($p < 0.05$), ★★ ($p < 0.005$), and ★★★ ($p < 0.001$). (b) Cell cycle analysis by FACS. The data represents mean ± SD of three individual experiments. The statistical significance was found out by comparing the control with different types of treated cells such as cells treated with blank NPs and suicide gene loaded NPs. The *p* values represent the same level of significance as described above. (c, d) FESEM images of a control cell and a cell treated with suicide gene loaded NPs (followed by treatment with 5-FC). The formation of the apoptotic bodies in the case of the treated cells was observed from the FESEM image. (e−g) Flow cytometric analyses via FITC conjugated annexin-V-propidium iodide (PI) staining in order to find out the apoptotic and necrotic populations (%). Here parts e, f, and g represent the control cells, cells treated with blank NPs and 5-FC, and cells treated with suicide gene loaded NPs and 5-FC, respectively. In the dot plots, the first, second, and third quadrants denote the live, early apoptotic (E.A.), and late apoptotic (L.A.) population of cells, respectively.

in its structure. On the other hand, the overall negative charge of pDNA would lead to polyplex formation due to electrostatic interaction between the two species.[57,58] This would lead to reduction in the zeta potential value of chitosan. The stability of the complex against DNase enzymatic action indicated its potential for DNA delivery. It may be mentioned here that, although viral vectors are used as efficient gene delivery vehicles, there are still concerns of their usage owing to immunogenicity and other biosafety issues. There are thus requirements of alternative methods of delivery of genes to

dx.doi.org/10.1021/am4051266 | ACS Appl. Mater. Interfaces 2014, 6, 712−724

affected tissues. In this context, use of chitosan and Au NCs in the form of composite NPs could be considered important, as they meet the criteria of size of the final complex, protection of DNA against digestion by nuclease, and possibly retaining structural integrity of the DNA. That the overall size of the polyplex was measured to be about 159 nm indicated their potential in gene delivery to cancer tissues preferentially to healthy ones.[59,60] This, however, needed to be tested.

The test for the potential of the composite NPs for gene delivery was carried out with *in vitro* delivery of the suicide gene (CD−UPRT) to human cervical cancer (HeLa) cells. In gene therapy, the emergence of cellular imaging by a fluorescent probe is convenient for real-time evaluation of the therapeutic approaches and their optimization.[61] As discussed before, the specificity of properties of the Au NCs makes their choice ideal for a probe, especially when embedded in a drug delivery vehicle. They also represent important replacement of conventional organic dyes, especially due to their photostability and high quantum yield. This was observed to be all the more interesting, as their multicolor emission allowed probe of cellular delivery of the composite NPs using flow cytometry. Thus, the delivery of gene loaded composite NPs to the cancer cells could be probed by using a FACS (fluorescence activated cell sorter), without the use of traditional dyes. When the cells were incubated with different amounts of gene-loaded Au NC−chitosan NPs for 4 h, a prominent shift of fluorescence intensity in FL3-H (low pass/670 nm) channels, which correspond to red fluorescence, was observed in comparison to signals of controls such as those of cells treated with only chitosan NPs and only gene-loaded chitosan NPs (i.e., without Au NCs) and cells in the absence of any treatment (refer to the Supporting Information, Figure S15c). It should be noted here that the shift of fluorescence intensity was maximum in the FL3-H channel which was comparatively less in the FL1-H channel (band-pass 530/30 nm) and much less in the FL2-H (band-pass 585/42 nm) channel. This was possibly due to the large Stokes shift of the metallic Au NC emission, as a blue laser (available in FACSCalibur, Ex. 488 nm) was used for excitation of the Au NCs (refer to the Supporting Information, Figure S15a−c). Further, two different doses of gene-loaded Au NC−chitosan NPs were used (50 and 75 μg mL^{-1}) for FACS analysis, upon which a gradual shift of fluorescence intensity in the FL3-H channel occurred, confirming the interaction of NPs with the cells (Figure 5a). Next, time-dependent FACS analysis revealed that fluorescence due to NCs could be followed for 8 h (Figure 5b). This suggests that Au NCs being delivered to the cells in the form of composite NPs were stable in the complex cell culture medium and the cellular environment. Thus, the NCs could indeed be used for probing mammalian cells and can compete with organic dyes as a new generation of robust cellular tracking agents.

The NP-mediated gene uptake was further supported by TEM analysis, where incorporation of the composite NPs with NCs in the cell was clearly observed (Figure 5f−i). The average size of the NC matched with the as-synthesized NCs, confirming not only the uptake of the particles but also retention of their structural integrity, which is essential for their role as support for theranostic devices. Interaction of gene-loaded NPs with cancer cells was further validated by microscopic studies. For that, HeLa cells were treated with gene loaded fluorescent composite NPs for 8 h followed by observation under an epi-fluorescence microscope, which Figure 5c−e showed the characteristic three color emissions of blue, green, and red due to Au NCs, when excited by UV, blue, and green light, respectively. Therefore, TEM, FACS, and optical microscopy experiments clearly demonstrated the delivery of composite NPs to cancer cells with retention of size and properties of the constituent NCs.

Considering that FACS experiments suggested transfection of HeLa cells, by NC and gene carrying composite NPs, it was deemed important to probe cell viability in order to appreciate the potential of gene therapy. It may be mentioned here that, although two different doses of gene-loaded Au NC−chitosan NPs were used (50 and 75 μg mL^{-1}) for FACS analysis in order to observe the gradual shift of the fluorescence with the increased concentration of the Au NCs, 50 μg mL^{-1} was used for the gene therapy. Thus, the ratio of pDNA and Au NC−chitosan NPs used for the gene transfection was 0.5:1 (w/w), as this formed the most stable polyplex. Following gene transfection, different doses of prodrug 5-FC were added to the transfected cells which were then incubated for 72 h. Subsequently, 3-(4,5-dimethylthiazolyl-2)-2,5-diphenyltetrazolium bromide (MTT) assay of the cells was performed. The assay revealed that the viability of the cells decreased gradually with increasing concentration of 5-FC as compared to control cells (Figure 6a). It is known that in the cells successfully transfected with CD−UPRT plasmid non-toxic prodrug 5-FC gets converted into toxic 5-FU by CD enzyme expressed by the plasmid. The toxic drug (5-FU) eventually kills the cell. That the cells were systematically annihilated upon treatment with the produg following NP delivery clearly established the merit of the drug delivery system. Further, the IC_{50} value of 5-FC (at which 50% of cells died) was found to be 14 ± 2.0 μg mL^{-1} 5-FC. This is consistent with the previously reported value, thus clearly supporting the validity of the approach.[55,62,63]

It would be worth mentioning here that apoptosis or "programmed cell death" is a common mechanism for exclusion of unwanted cells from the body and is generally a preferred mode of cell death pursued by treatment of any therapeutic agent, whereas necrosis is the sudden death of cells. In order to have an idea of the mechanism of cell death involved in the present case, cell cycle analysis by propidium iodide (PI) staining was performed, which showed that the cell populations in different phases of the cell cycle (G0/G1, S, and G2/M) remained unaffected (Figure 6b), after treatment with suicide gene (as was present in the composite NP), as compared to their respective controls. However, a significant increase in sub-G0/G1 population (relating to the apoptotic population) was observed in cells treated with suicide genes (7.1 ± 1.6%), which was the primary signature of the apoptosis as the mode of cell death (further details are available in the Supporting Information, Figure S16). Treated cells were further examined under FESEM (Figure 6c,d), which substantiated the formation of apoptotic bodies. Another important point needed to be addressed is that the mode of cell death was primarily due to apoptosis, not necrosis. For this, a FITC conjugated annexin-V-PI double staining experiment was performed and was probed by using FACS (Figure 6e−g). The FACS results illustrated that in the present case, due to functional expression of suicide genes, there was a substantial number of cell population in early (3.7 ± 0.8%) and late apoptotic (5.5 ± 0.9%) stages, as compared to the necrotic population (2.1 ± 0.1%) (refer to the Supporting Information, Figure S17). Moreover, the total apoptotic cells in the early and late stages were found to be ∼9.2%, which was similar to the sub-G0/G population observed in PI staining. Overall, the experiments revealed

that use of NC containing NPs in suicide gene delivery to cancer cells was effective in carrying out "programmed cell death". The NP-mediated gene uptake—which resulted in apoptosis—also indicated that the fluorescence microscopic images observed herein were possibly due to internalization of the composite NPs, rather than NPs being present on the cell surface. The above results in conjunction with the results from the Au NC based fluorescence microscopy and FACS studies clearly indicated the competitive edge of the use of fluorescent Au NCs over organic dyes in probing the effects of gene prodrug delivery to cancer cells. Also, the current method of synthesis of Au NCs being embedded in chitosan, which can easily be converted into nanocarriers, creates a new concept in theranostics and brings in new ideas in cancer therapy.

CONCLUSION

In a nutshell, we have developed a fast and easy aqueous method of synthesis of highly fluorescent, RGB emitting Au NCs by using chitosan (in combination with MPA) as reducing and stabilizing agents. The Au NCs in chitosan were stable in the aqueous phase as well as in solid powder. Results also indicated that surface property or ligand, other than size of the NC, was important in the origin and reversible tuning of fluorescence at different pH's of the medium. The use of chitosan helped in the facile formation of composite NPs, which was useful for drug delivery to cancer cells in conjunction with easy imaging. Further, the advantage of emission of three basic colors (RGB) was useful in imaging cells while therapy was being pursued. Additionally, they helped in FACS analysis without the use of additional dyes. Chitosan NPs have been widely employed as suitable gene carriers; however, in the present case, the fluorescent property of the delivery vehicle helped in direct evaluation of suicide gene delivery, by performing either FACS or microscopy study. This current method of formation of fluorescent NCs and their use in theranostic application bring in a new approach in modern nanotechnology-based drug delivery. This is expected to augment as well as alter conventional approaches in gene therapy and other drug-based therapeutics.

ASSOCIATED CONTENT

Supporting Information

Further experimental details and figures, calculation of the quantum yield, formation of film, MALDI-TOF data, photostability data, FTIR spectra, cell cycle analysis, and FESEM images. This material is available free of charge via the Internet at http://pubs.acs.org.

AUTHOR INFORMATION

Corresponding Authors

*E-mail: sghosh@iitg.ernet.in.
*E-mail: arun@iitg.ernet.in.

Notes

The authors declare no competing financial interest.

ACKNOWLEDGMENTS

This research was supported by the Department of Biotechnology (Nos. BT/49/NE/TBP/2010 and BT/01/NE/PS/08). Assistance from the Central Instruments Facility (CIF), IIT Guwahati for TEM (sponsored partly by DST, Govt. of India), and FESEM is gratefully acknowledged.

REFERENCES

(1) Zheng, J.; Nicovich, P. R.; Dickson, R. M. *Annu. Rev. Phys. Chem.* **2007**, *58*, 409−431.
(2) Shang, L.; Dong, S.; Nienhaus, G. U. *Nano Today* **2011**, *6*, 401−418.
(3) Varnavski, O.; Ramakrishna, G.; Kim, J.; Lee, D.; Goodson, T. *J. Am. Chem. Soc.* **2010**, *132*, 16−17.
(4) Shibu, E. S.; Muhammed, M. A. H.; Tsukuda, T.; Pradeep, T. *J. Phys. Chem. C* **2008**, *112*, 12168−12176.
(5) Wu, Z.; Jin, R. *Nano Lett.* **2010**, *10*, 2568−2573.
(6) Hong, S.; Shafai, G.; Bertino, M.; Rahman, T. S. *J. Phys. Chem. C* **2011**, *115*, 14478−14487.
(7) Wang, H.-H.; Lin, C.-A. J.; Lee, C.-H.; Lin, Y.-C.; Tseng, Y.-M.; Hsieh, C.-L.; Chen, C.-H.; Tsai, C.-H.; Hsieh, C.-T.; Shen, J.-L.; et al. *ACS Nano* **2011**, *5*, 4337−4344.
(8) Tian, D.; Qian, Z.; Xia, Y.; Zhu, C. *Langmuir* **2012**, *28*, 3945−3951.
(9) Retnakumari, A.; Setua, S.; Menon, D.; Ravindran, P.; Muhammed, H.; Pradeep, T.; Nair, S.; Koyakutty, M. *Nanotechnology* **2010**, *21*, 055103.
(10) Zhang, J.; Fu, Y.; Conroy, C. V.; Tang, Z.; Li, G.; Zhao, R. Y.; Wang, G. *J. Phys. Chem. C* **2012**, *116*, 26561−26569.
(11) Valden, M.; Lai, X.; Goldman, D. W. *Science* **1998**, *281*, 1647−1650.
(12) Turner, M.; et al. *Nature* **2008**, *454*, 981−983.
(13) Gao, Y.; Shao, N.; Pei, Y.; Zeng, X. C. *Nano Lett.* **2010**, *10*, 1055−1062.
(14) O'Neill, P. R.; Young, K.; Schiffels, D.; Fygenson, D. K. *Nano Lett.* **2012**, *12*, 5464−5469.
(15) Wen, X.; Yu, P.; Toh, Y.-R.; Hsu, A.-C.; Lee, Y.-C.; Tang, J. *J. Phys. Chem. C* **2012**, *116*, 19032−19038.
(16) Guével, X. Le; Hötzer, B.; Jung, G.; Hollemeyer, K.; Trouillet, V.; Schneider, M. *J. Phys. Chem. C* **2011**, *115*, 10955−10963.
(17) Xie, J.; Zheng, Y.; Ying, J. Y. *J. Am. Chem. Soc.* **2009**, *131*, 888−889.
(18) Schaeffer, N.; Tan, B.; Dickinson, C.; Rosseinsky, M. J.; Laromaine, A.; McComb, D. W.; Stevens, M. M.; Wang, Y.; Petit, L.; Barentin, C.; et al. *Chem. Commun.* **2008**, 3986−3988.
(19) Wei, H.; Wang, Z.; Yang, L.; Tian, S.; Hou, C.; Lu, Y. *Analyst* **2010**, *135*, 1406−1410.
(20) Liu, G.; Shao, Y.; Ma, K.; Cui, Q.; Wu, F.; Xu, S. *Gold Bull.* **2012**, *45*, 69−74.
(21) Pettibone, J. M.; Hudgens, J. W. *ACS Nano* **2011**, *5*, 2989−3002.
(22) Duan, H.; Nie, S. *J. Am. Chem. Soc.* **2007**, *129*, 2412−2413.
(23) Lin, C.-A. J.; Yang, T.-Y.; Lee, C.-H.; Huang, S. H.; Sperling, R. A.; Zanella, M.; Li, J. K.; Shen, J.-L.; Wang, H.-H.; Yeh, H.-I.; et al. *ACS Nano* **2009**, *3*, 395−401.
(24) Wu, Z.; Suhan, J.; Jin, R. *J. Mater. Chem.* **2009**, *19*, 622−626.
(25) Zhang, H.; Huang, X.; Li, L.; Zhang, G.; Hussain, I.; Li, Z.; Tan, B. *Chem. Commun.* **2012**, *48*, 567−569.
(26) Qian, H.; Jin, R. *Chem. Mater.* **2011**, *23*, 2209−2217.
(27) Schaaff, T. G.; Whetten, R. L. *J. Phys. Chem. B* **1999**, *103*, 9394−9396.
(28) Sanpui, P.; Chattopadhyay, A.; Ghosh, S. S. *ACS Appl. Mater. Interfaces* **2011**, *3*, 218−228.
(29) Vassaux, G.; Martin-Duque, P. *Expert Opin. Biol. Ther.* **2004**, *4*, 519−530.
(30) Calvo, P.; Remunan-Lopez, C.; Vila-Jato, J. L.; Alonso, M. J. *J. Appl. Polym. Sci.* **1997**, *63*, 125−132.
(31) Negishi, Y.; Tsukuda, T. *Chem. Phys. Lett.* **2004**, *383*, 161−165.
(32) Lebedkin, S.; Langetepe, T.; Sevillano, P.; Fenske, D.; Kappes, M. M. *J. Phys. Chem. B* **2002**, *106*, 9019−9026.
(33) Luo, Z.; Yuan, X.; Yu, Y.; Zhang, Q.; Leong, D. T.; Lee, J. Y.; Xie, J. *J. Am. Chem. Soc.* **2012**, *134*, 16662−16670.
(34) Yuan, X.; Luo, Z.; Zhang, Q.; Zhang, X.; Zheng, Y.; Lee, J. Y.; Xie, J. *ACS Nano* **2011**, *5*, 8800−8808.
(35) Qian, H.; Zhu, Y.; Jin, R. *ACS Nano* **2009**, *3*, 3795−3803.

(36) Yu, Y.; Luo, Z.; Yu, Y.; Lee, J. Y.; Xie, J. *ACS Nano* **2012**, *6*, 7920−7927.
(37) Jhaveri, S. D.; Foos, E. E.; Lowy, D. A.; Chang, E. L.; Snow, A. W.; Ancona, M. G. *Nano Lett.* **2004**, *4*, 737−740.
(38) Murayama, H.; Narushima, T.; Negishi, Y.; Tsukuda, T. *J. Phys. Chem. B* **2004**, *108*, 3496−3503.
(39) Schaaff, T. G.; Knight, G.; Shafigullin, M. N.; Borkman, R. F.; Whetten, R. L. *J. Phys. Chem. B* **1998**, *102*, 10643−10646.
(40) Zheng, J.; Zhang, C.; Dickson, R. *Phys. Rev. Lett.* **2004**, *93*, 077402-1−077402-4.
(41) Guével, X.; Le Trouillet, V.; Spies, C.; Li, K.; Laaksonen, T.; Auerbach, D.; Jung, G.; Schneider, M. *Nanoscale* **2012**, *4*, 7624−7631.
(42) Xavier, P. L.; Chaudhari, K.; Baksi, A.; Pradeep, T. *Nano Rev.* **2012**, *3*, 14767.
(43) Xu, H.; Suslick, K. S. *ACS Nano* **2010**, *4*, 3209−3214.
(44) Shen, Z.; Duan, H. W.; Frey, H. *Adv. Mater.* **2007**, *19*, 349−352.
(45) Shang, L.; Dong, S. J. *Chem. Commun.* **2008**, *9*, 1088−1090.
(46) Medintz, I. L.; Uyeda, H. T.; Goldman, E. R.; Mattoussi, H. *Nat. Mater.* **2005**, *4*, 435−446.
(47) Stürzenbaum, S. R.; Höckner, M.; Panneerselvam, A.; Levitt, J.; Bouillard, J.-S.; Taniguchi, S.; Dailey, L.-A.; Khanbeigi, R. A.; Rosca, E. V.; Thanou, M.; et al. *Nat. Nanotechnol.* **2013**, *8*, 57−60.
(48) Chang, Y.-P.; Pinaud, F.; Antelman, J.; Weiss, S. *J. Biophotonics* **2008**, *1*, 287−298.
(49) Chan, W.; Shiao, N. *Acta Pharmacol. Sin.* **2008**, *29*, 259−266.
(50) Peer, D.; Karp, J. M.; Hong, S.; Farokhzad, O. C.; Margalit, R.; Langer, R. *Nat. Nanotechnol.* **2007**, *2*, 751−760.
(51) Kamaly, N.; Xiao, Z.; Valencia, P. M.; Radovic-Moreno, A. F.; Farokhzad, O. C. *Chem. Soc. Rev.* **2012**, *41*, 2971−3010.
(52) Davis, M. E.; Chen, Z. (Georgia); Shin, D. M. *Nat. Rev. Drug Discovery* **2008**, *7*, 771−782.
(53) Ruoslahti, E.; Bhatia, S. N.; Sailor, M. J. *J. Cell Biol.* **2010**, *188*, 759−768.
(54) Kaliberov, S. A.; Chiz, S.; Kaliberova, L. N.; Krendelchtchikova, V.; Della Manna, D.; Zhou, T.; Buchsbaum, D. J. *Cancer Gene Ther.* **2006**, *13*, 203−214.
(55) Gopinath, P.; Ghosh, S. S. *Biotechnol. Lett.* **2008**, *30*, 1913−1921.
(56) Huang, Y. H.; et al. *Cancer Res.* **2009**, *69*, 6184−6191.
(57) Han, L.; Zhao, J.; Zhang, X.; Cao, W.; Hu, X.; Zou, G.; Duan, X.; Liang, X.-J. *ACS Nano* **2012**, *6*, 7340−7351.
(58) Lee, D.; Mohapatra, S. S. *Methods Mol. Biol.* **2008**, *433*, 127−140.
(59) Lu, F.; Wu, S.-H.; Hung, Y.; Mou, C.-Y. *Small* **2009**, *5*, 1408−1413.
(60) Kim, J.-H.; Kim, Y.-S.; Park, K.; Lee, S.; Nam, H. Y.; Min, K. H.; Jo, H. G.; Park, J. H.; Choi, K.; Jeong, S. Y.; et al. *J. Controlled Release* **2008**, *127*, 41−49.
(61) Bogdanov, A., Jr.; Weissleder, R. *Trends Biotechnol.* **2002**, *20*, S11−S18.
(62) Gopinath, P.; Ghosh, S. S. *Mol. Biotechnol.* **2008**, *39*, 39−48.
(63) Kawamura, K.; et al. *Cancer Gene Ther.* **2000**, *7*, 637−643.